Calcif Tissue Int (1992) 51:443–448

Calcified Tissue International

FT-IR Microscopic Mappings of Early Mineralization in Chick Limb Bud Mesenchymal Cell Cultures

Adele L. Boskey,[1] Nancy Pleshko Camacho,[2] Richard Mendelsohn,[2] Stephen B. Doty,[1] and Itzhak Binderman[1]

[1]Laboratory for Ultrastructure Biochemistry, The Hospital for Special Surgery, 535 East 70th Street, affiliated with Cornell University Medical College, New York, New York 10021; and [2]Department of Chemistry, Rutgers University, Newark, New Jersey, USA

Received October 18, 1991, and in revised form December 26, 1991

Summary. Chick limb bud mesenchymal cells differentiate into chondrocytes and form a cartilaginous matrix in culture. In this study, the mineral formed in different areas within cultures supplemented with 4 mM inorganic phosphate, or 2.5, 5.0, and 10 mM β-glycerophosphate (βGP), was characterized by Fourier-transform infrared (FT-IR) microscopy. The relative mineral-to-matrix ratios, and distribution of crystal sizes at specific locations throughout the matrix were measured from day 14 to day 30. The only mineral phase detected was a poorly crystalline apatite. Cultures receiving 4 mM inorganic phosphate had smaller crystals which were less randomly distributed around the cartilage nodules than those in the βGP-treated cultures. βGP-induced mineral consisted of larger, more perfect apatite crystals. In cultures receiving 5 or 10 mM βGP, the relative mineral-to-matrix ratios (calculated from the integrated intensities of the phosphate and amide I bands, respectively) were higher than in the cultures with 4 mM inorganic phosphate or in the *in vivo* calcified chick cartilage.

Key words: Hydroxyapatite – Mineralization – Cartilage calcification – FTIR – Infrared spectroscopy.

Chick limb bud mesenchymal cells from stage 21–24 embryos when plated in a micromass culture system [1] produce a mineralizable matrix [2–5]. Mineralization, detectable by histochemical stains, occurs around individual cartilage nodules and on the periphery of the culture when the media is supplemented with additional phosphate [2, 5]. Characterization of the mineral by wide-angle X-ray diffraction of pulverized cultures has shown the presence of a poorly crystalline apatite in cultures supplemented with 4 mM inorganic phosphate [4, 5]. When 2.5–10 mM β-glycerophosphate (βGP) was added to the cultures in place of inorganic phosphate, as is generally done by investigators studying mineralization in culture, larger/more perfect crystals were detected by X-ray diffraction [5], even when the media phosphate concentration was comparable (5 mM Pi versus 5 mM βGP). Histochemical staining indicated that the mineral distribution varied with time and location [2, 5]. The nature of the spatial variation is difficult to assess by X-ray powder diffraction which requires grinding and pooling of the entire culture. Electron microscopy has the potential to address the variation, but requires numerous samples, and even for these, the spatial resolution relative to the whole culture is lost.

Fourier-transform infrared (FT-IR) microscopy has previously been used to map the changes in the mineral properties of the growth plate [6] and normal and diseased bone [7–9] at 20 μm resolution. The spectrum at each site, characteristic of those reported for mineralized tissues by numerous investigators (e.g., [10–14]), not only provides "fingerprint" identification of the mineral phase, but it can also be analyzed mathematically to provide information about the constituent bands [8, 9, 15]. The positions and widths of subbands contributing to the predominant apatite phosphate absorption at 800–1200 cm^{-1} can be correlated with alterations in crystal lengths calculated from X-ray diffraction line-broadening analyses of model calcium phosphate compounds whose crystal lengths are in the size range of biologic apatites [15]. Such empirical procedures facilitate interpretation of spectra of biologic apatites.

The purpose of the present investigation was to map the changes in the mineral properties of mineralizing chick limb bud mesenchymal cell cultures using FT-IR microscopy in order to determine how the mineral changed with site and time, and whether any nonapatitic phases were present.

Materials and Methods

Culture Technique

The culture conditions used for these studies were previously established to give a matrix resembling the physiologic calcified cartilage of the chick [5]. In brief, stage 21–24 White Leghorn chick embryos were cultured in media containing 1.1 mM Ca^{+2}, 1 mM inorganic phosphate (Pi), 25 μg/ml vitamin C, antibiotics, and glutamine. At day 2, either 3 mM Pi, 2.5, 5, or 10 mM βGP was added to all but control dishes. Phosphate, glutamine, and vitamin C supplementation was continued with each additional media change (every other day). The Ca [16] and inorganic phosphate [17] concentrations in the media were monitored throughout the 30-day course of the experiment.

At days 14, 17, 21, and 30, representative cultures were saved for electron microscopic examination (for details of specimen handling see [5]), or X-ray diffraction analyses, and the remainder were fixed in 100% ethanol on glass slides to facilitate transfer to a barium fluoride FT-IR window. In some cases the cultures were transferred from the incubator directly, lifting the spot culture from the dish and placing it onto the FT-IR window, blotting the medium dry, and placing a second window on top of the culture to flatten it for FT-IR examination. Spectra were collected within 30 minutes of the time of transfer to avoid changes due to cell death.

FT-IR microscopic examination of the cultures were recorded on either a Mattson-Sirius FT-IR microscope equipped with a Mercury-

Offprint requests to: A. L. Boskey

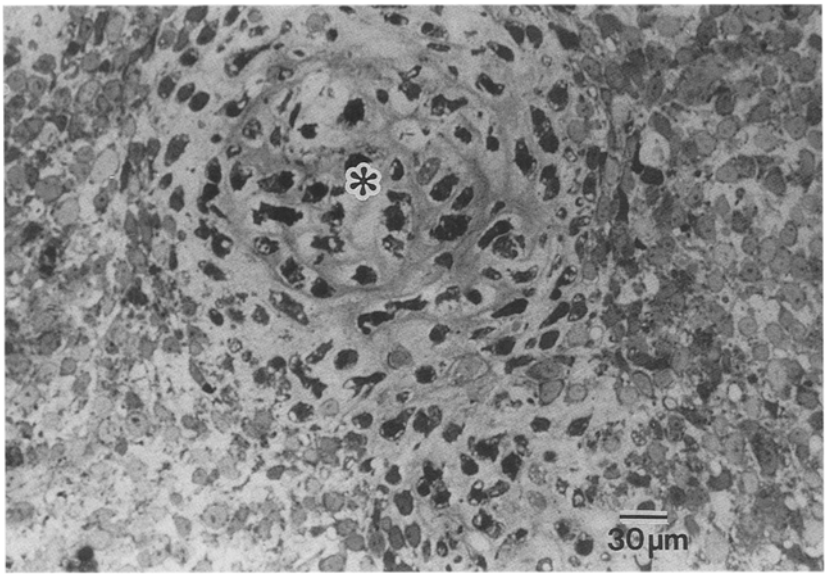

Fig. 1. Toluidine blue-stained thick section of a day 21 culture developed in the presence of 4 mM Pi. The center of the cartilage nodule is labeled with an asterisk.

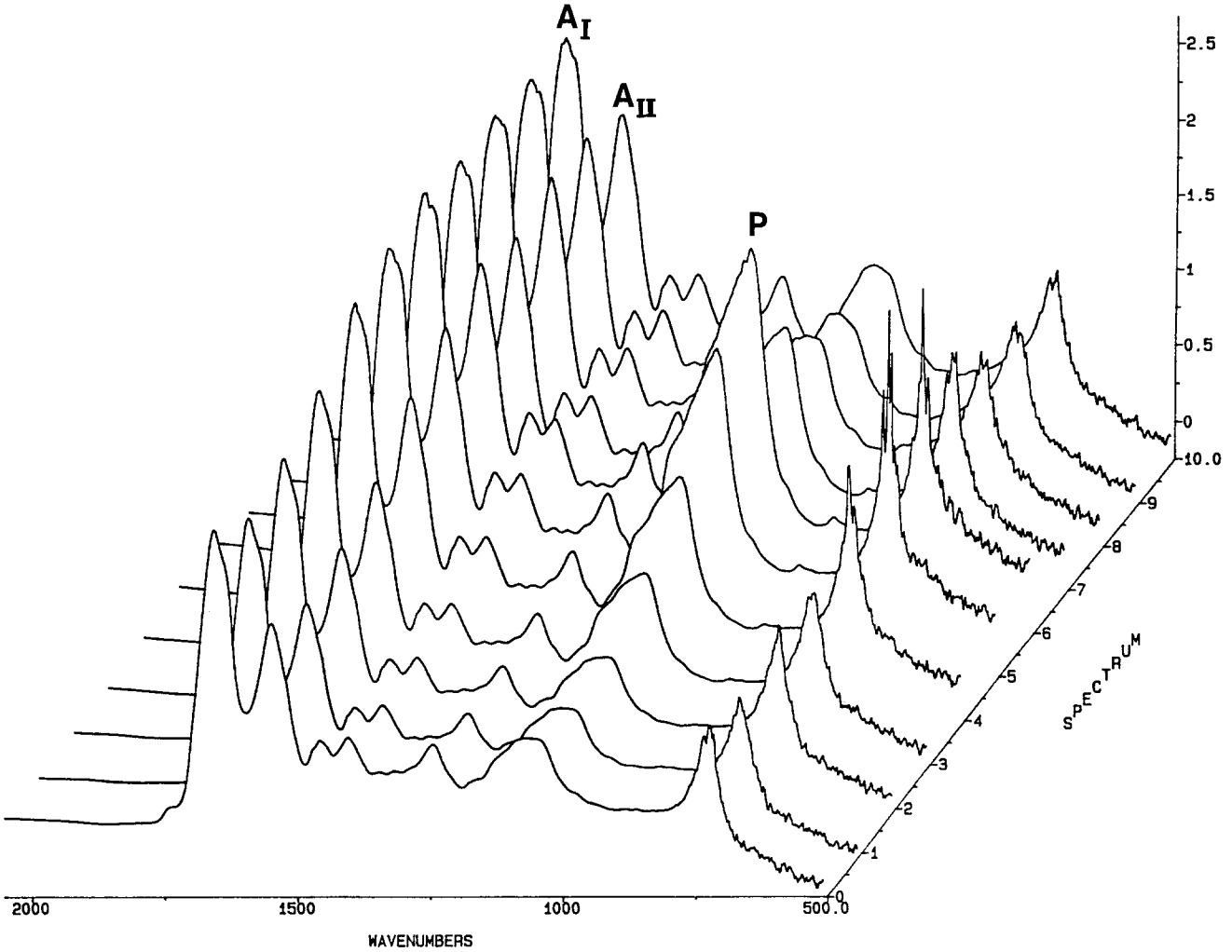

Fig. 2. Map of the FT-IR spectra of a 21-day culture developed in the presence of 5 mM βGP. Note that the relative intensity of the amide I (A_I) and amide II (A_{II}) peaks do not change, whereas the phosphate peak of the mineral (P) varies markedly. Starting at the center of the nodule (spectrum 1), little mineral is present. The intensity of the mineral peak increases while the peak changes in shape as the distance from the center of the nodule increases, peaking at 40 μm (spectrum 6), and decreasing again with further distance from the nodule.

Cadmium-Telluride detector (Madison, WI) or on a Spectra-Tech (Stamford, CT) IRμS microspectrometer (ethanol-fixed cultures only). Routinely, 256 interferograms were collected, co-added, apodized with a triangular function, and fast Fourier transformed to yield spectra with 4 cm^{-1} resolution with data encoded every 2 cm^{-1}.

At least three different nodules and three different sites along the periphery (edge) of the culture were examined for each of three ethanol-fixed cultures at each time point. Spectra were recorded at approximately 20 μm intervals starting from the center of each nodule or at 20 μm intervals from the edge of the culture. These spectra were compared with spectra from cryosections of 17-day-old embryonic chick calcified and noncalcified cartilage.

Analyses of the spectra, including calculation of integrated areas, subtractions, and curve fitting were performed using a series of integrated programs kindly provided by Doug Moffatt (National Research Council of Canada). A total of 109 spectra were analyzed. First, following base-line definition, relative mineral-to-matrix ratios (PO_4/protein) were calculated as the ratio of the integrated area of the phosphate band (900–1200 cm^{-1}) to that of the Amide I band (1580–1705 cm^{-1}). As the relative ratios of the amide I and amide II bands were relatively constant, it was assumed that the contribution of the water band at 1640 cm^{-1} was negligible.

Control, nonmineralizing cultures, obtained at the same time points as the culture whose spectra was being analyzed, were then used for spectral subtraction. The subtractions were performed minimizing the amide I band. The phosphate ν_1 and ν_3 regions, 900–1200 cm^{-1}, were analyzed using a curve-fitting algorithm, and data correlated with crystallite size using an equation derived from X-ray and FT-IR analyses of synthetic and biologic apatites 100–200 Å in length [15]. (Throughout this text, the term "crystal size" will be used to indicate the length of the crystal in the direction parallel to the c-axis of the unit cell as determined by X-ray diffraction line-broadening analysis. This parameter reflects both the actual size and the perfection of the crystal.)

As previously demonstrated, the ν_1, ν_3 contour was composed of three main and three minor subbands. The percent area of a component near 1060 cm^{-1}, which decreases as the length of the apatite crystal (as determined by X-ray diffraction [15]) increases, was used to provide an estimate of crystallite size. The position of the major band near 1020 cm^{-1}, which increases with increasing length of the apatite crystal, provided a confirmation of the previous result.

In all figures, replicate analyses are expressed as mean ± SD, and statistically significant differences were calculated using the Student's *t* test.

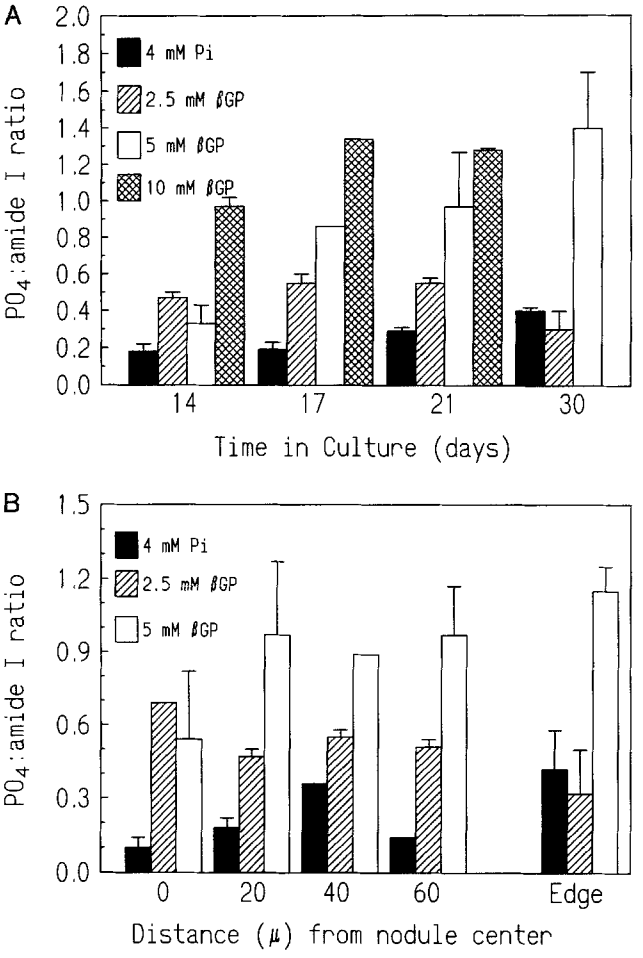

Fig. 3. Relative phosphate to amide I ratios in mineralizing cultures. **(A)** Changes in ratio of phosphate to amide I integrated intensities at a site 20 μm from the center of the nodule as a function of time in culture. **(B)** Relative phosphate to amide I ratios as a function of distance from the center of the nodule at day 21. All values are mean ± SD for n > 3 cultures.

Results

Figure 1 is a light micrograph of a Toluidine blue stained culture, developed in the presence of 4 mM Pi, showing a typical cartilage nodule and the surrounding matrix. Typical spectra taken from the center of one nodule out to 150 μm from that site are shown in Figure 2. This figure was obtained using a mapping module, and presents the relative intensities of the protein (amide I and II bands) and the phosphate band at 900–1070 cm^{-1}. It should be noted in this figure that the contributions from the protein remain relatively constant throughout the distance scanned. In contrast, the relative amount of mineral (indicated by the integrated intensity of phosphate band) increases and then decreases as the center of the nodule is approached. The shape of the phosphate band also varies with distance from the center of the nodule. These spectra were neither subtracted nor curve-fit, and hence represent the total data obtained. Comparisons of these spectra with those of model compounds [6, 8, 10] showed the best agreement with a poorly crystalline hydroxyapatite.

Figure 3 summarizes the change in relative mineral-to-matrix ratios under different culture conditions. Examining a site ~20 μm from the center of the nodule (Fig. 3A), the amount of mineral can be seen to increase with time in culture, the greatest accumulation occurring in those cultures with 5 and 10 mM βGP. Spectra with 10 mM βGP could not be mapped by day 30 because the nodules were totally obscured by mineral. In fact, some of the ratios in the presence of βGP exceed the 0.5–1.5 ratios observed for chick calcified cartilage. At a single time point (e.g., 21 days) in the presence of inorganic phosphate, there was a significant site-to-site variation in relative mineral-to-matrix ratio. In contrast, as is illustrated in Figure 3B, cultures with βGP contained more mineral, but this mineral was randomly dispersed. As is indicated in this figure, the relative mineral-to-matrix ratio was larger, but, as indicated by the scatter in the data, more variable around the periphery (edge) of the micromass culture. These findings agree well with the electron microscopic observations in which the βGP-treated cultures appeared to have a much more abundant, albeit more random distribution of mineral (Fig. 4).

A typical spectrum for chick calcified cartilage is presented in Figure 5. The amide I and II peaks are noisy due to the water vapor in the cryosections, but the similarity of the spectra to those in the mineralized cultures seen in Figure 2 is apparent.

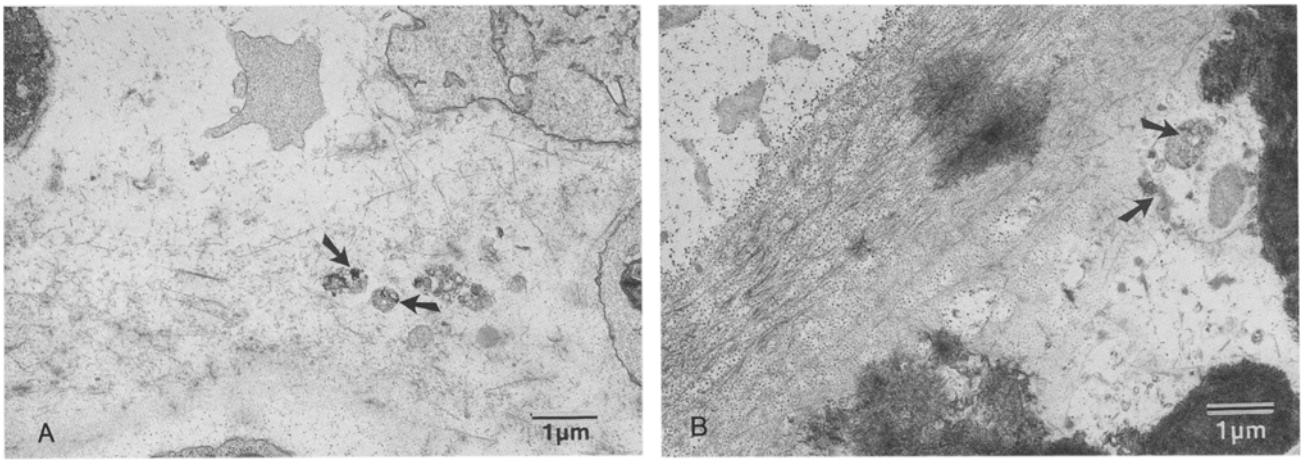

Fig. 4. Electron micrographs of cultures at day 21. (**A**) Culture with 4 mM Pi. Mineral deposits indicated by arrows. (**B**) Culture with 5 mM βGP. Note the random distribution of the mineral and cellular debris which contain mineral (arrows). Bar = 2 μm.

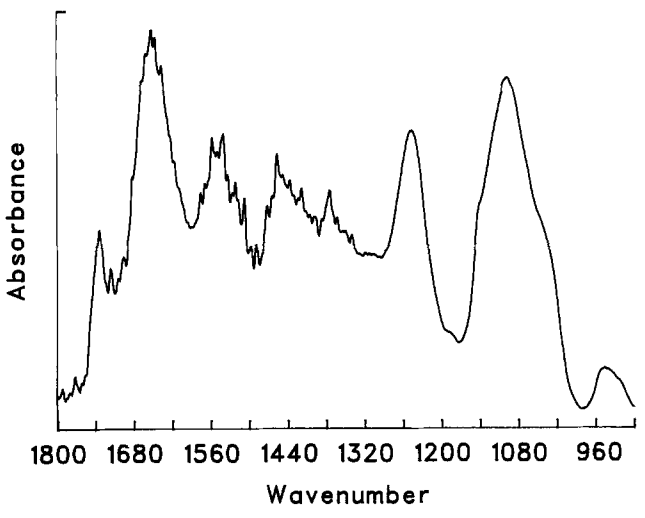

Fig. 5. FT-IR spectra of calcified cartilage from a 17-day-old chick embryo's femur.

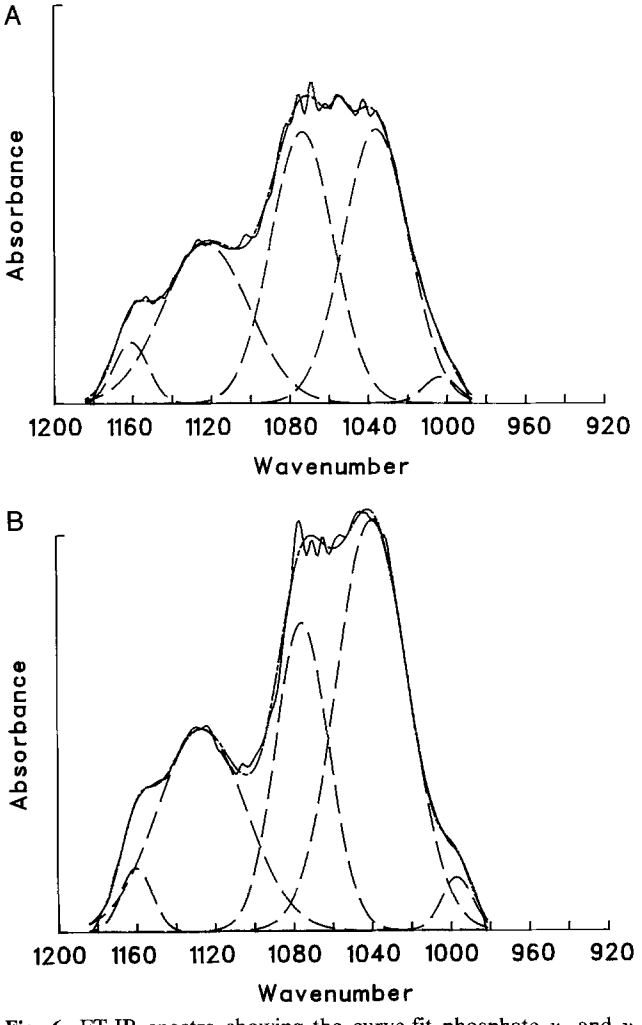

Fig. 6. FT-IR spectra showing the curve-fit phosphate ν_1 and ν_3 regions, 900–1200 cm^{-1} of (**A**) a 30-day culture maintained in the presence of 4 mM Pi, and (**B**) a 21-day culture maintained in the presence of 2.5 mM βGP. Subbands smaller than 5% in area do not appear on this figure. The height of the y-axes for both figures is identical. Spectra have been baseline flattened between the indicated points.

Typical curve fit spectra for the ν_1, ν_3 contour in cultures with 4 mM Pi and 2.5 mM βGP are presented in Figure 6A and B. The points of zero absorbance constitute the baseline after redrawing. The components of the 900–1200 cm^{-1} band were calculated using an iterative algorithm which varies the ratio of lorentzian and gaussian components and adjusts the peak positions. Iterations were continued until the goodness of fit was $\leq 10^{-3}$ and no additional changes in goodness of fit were obtained. By day 30 in the presence of Pi, the overall contour of the band (Fig. 6A) was comparable to that at day 21 in the presence of 2.5 mM βGP (Fig. 6B). However, of the major subbands, the component at ~1070 cm^{-1} was greater in area in the Pi culture, whereas the ~1020 cm^{-1} was at a lower position than that in the βGP culture. The crystal length at different sites within the same culture and in different cultures was determined using the previously published equation [15] which correlates the percentage area of the major subband at 1060–1080 cm^{-1} with the crystal length measured by X-ray diffraction.

Figure 7 presents a summary of the changes in the mineral as a function of time and culture condition, showing the

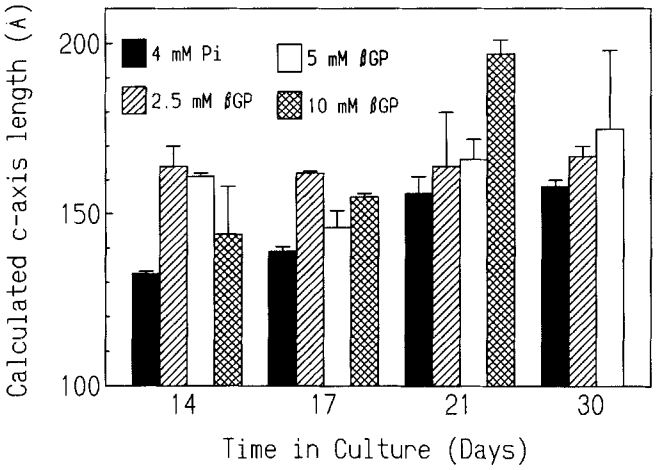

Fig. 7. Calculated crystal length as function of culture time and conditions. Mean ± SD for n > 3 cultures. (**A**) Variation with time in culture, calculations based on spectra take 20 μm from center of nodule.

time-dependent changes measured at 20–40 μm from the center of the nodule. The spectra obtained for the fresh specimens, after subtraction and curve-fitting, were superimposable on those for ethanol-fixed specimens (not shown), and thus data from all are combined. As can be seen in this figure, in the presence of 4 mM Pi, the mineral crystal size (which also is an indication of crystal perfection), increased gradually with time. With βGP the crystals on average started out larger, and the size distribution was more random.

Discussion

Infrared and FT-IR analyses have been widely used to characterize apatite mineral, both in tissues (e.g., [6–9, 11–13]) and synthetics (e.g., [10, 13–15]). The coupling of a light microscope to the FT-IR spectrometer has facilitated mapping of changes in mineral quality and quantity in normal and rachitic rat growth plates [6]. Now, the application of this technique to mineral formed in culture has allowed for the determination of the spatial variation in mineral-to-protein ratio, and the characterization of the effect of different culture conditions on the properties of the mineral.

As in the X-ray diffraction analysis [4, 5], the FT-IR analyses of the mineralizing cultures showed no evidence of any crystalline calcium phosphate phase other than a poorly crystalline apatite. FT-IR spectra characteristic of other phases [6], proposed as precursors in the formation of hydroxyapatite (amorphous calcium phosphate [18], octacalcium phosphate [12], brushite [19]) were not observed. These data suggest that at least for cartilage calcification *in vitro*, a poorly crystalline apatite is the predominant phase formed. Although it might be argued that the ethanol fixation and drying caused the disappearance of precursor phases, the observation that the unfixed tissues gave the same curve-fit spectra as those processed in ethanol, and our data on the effects of ethanol fixation on the mineral spectra [9] suggest that this is not the case.

With time in culture, in the presence of 4 mM Pi, there is growth and/or perfection of the mineral crystals, as reflected by the calculated crystal length. In the presence of βGP, though some of the mineral around the nodules still appears physiologic in size, the mineral in the periphery of the culture appears to have crystals that are larger/more perfect than those in calcified cartilage in the animal. The formation of larger crystals in βGP-treated cultures is probably due to the concentration gradients that develop as the glycerophosphate is hydrolyzed by membrane-bound enzymes such as alkaline phosphatase [20]. Not all mineralizing culture systems require βGP [5, 20, 21], and cells that do not produce mineralizable matrices can similarly be made to mineralize by the addition of βGP and alkaline phosphatase [22]. Because the mineral formed when βGP is added to the mesenchymal cell cultures, because of its increased size/perfection, appears to be less like the mineral formed in the animal than the smaller crystals formed when inorganic phosphate is added to the cultures [5], it is suggested that βGP supplementation of such cultures may not be appropriate.

The formation of larger/more perfect crystals in the presence of βGP was indicated by the X-ray diffraction data [5], but for the X-ray analyses it was not possible to detect the spatial distribution of different-sized crystals. Although currently we are limited by the spatial resolution of the instrument and the absence of other quantitative correlations between the subband structure and the mineral structure, the FT-IR microscopic method promises to be an important additional tool that can help elucidate the events in the calcification process.

Acknowledgments. The authors would like to express their appreciation to the staff of Spectra-Tek for the use of their FT-IR microscope, and to Ms Dalina Stiner and Ms Kitty Bock for their technical assistance. This work was supported by NIH Grant AR 37661.

References

1. Ahrens PBA, Solursh M, Reiter RS (1977) Stage-related capacity for limb chondrogenesis in cell culture. Dev Biol 60:69–82
2. Binderman I, Green RM, Pennypacker JP (1979) Calcification of differentiating skeletal mesenchyme in vitro. Science 206:222–225
3. Solursh M (1987) Use of tissue culture in the analysis of limb chondrogenesis. Mechanistic approaches to developmental toxicology. In: McLachlin JM, Pratt RM, Marker CL (ed) Developmental toxicology: mechanisms and risk, Banbury Report no 26. Cold Spring Harbor Laboratory, New York
4. Boskey AL, Stiner D, Doty S, Binderman I (1991) Requirement of vitamin C for cartilage calcification in a mesenchymal cell culture. Bone 12:277–282
5. Boskey AL, Stiner D, Leboy P, Doty S, Binderman I (1992) Optimal conditions for cartilage calcification in differentiating chick limb-bud mesenchymal cells. Bone Miner 16:11–37
6. Mendelsohn R, Hassankhani A, DiCarlo E, Boskey A (1989) FT-IR microscopy of endochondral ossification at 20 μ spatial resolution. Calcif Tissue Int 44:20–24
7. Boskey AL (1990) Bone mineral and matrix: are they altered in osteoporosis? Orthop Clin North Am 21:19–29
8. Pleshko NL (1991) Applications of FTIR microscopy to biomineralization. PhD Thesis, Rutgers University, Newark NJ
9. Pleshko NL, Boskey AL, Mendelsohn R (in press) An FTIR investigation of the effect of tissue preservation on bone. Calcif Tissue Int 51:72–77
10. Bailey RT, Holt C (1989) Fourier transform infrared spectroscopy and characterization of biological calcium phosphates. In: Hukins DWL (ed) Calcified tissue. Macmillan Press Ltd, Houndmills, Basingstoke, Hampshire, pp 93–120
11. Rey C, Lian JB, Grynpas M, Shapiro F, Zylerberg L, Glimcher MJ (1989) Non-apatitic environments in bone mineral. FT-IR detection, biological properties, and changes in several disease states. Connect Tissue Res 21:267–273

12. Sauer GR, Wuthier RE (1988) Fourier transform infrared characterization of mineral phases formed during induction of mineralization by collagenase-released matrix vesicles. J Biol Chem 263:13718
13. Termine JD, Lundy DR (1973) Hydroxide and carbonate in rat bone mineral and its synthetic analogues. Calcif Tissue Res 13:73–82
14. Termine JD, Lundy DR (1974) Vibrational spectra of some phosphate salts amorphous to x-ray diffraction. Calcif Tissue Res 15:55–70
15. Pleshko NL, Mendelsohn R, Boskey A (1991) A novel IR spectroscopic method for the determination of crystallinity of hydroxyapatite minerals. Biophys J 60:786–793
16. Willis JB (1960) Determination of metals in blood serum by atomic absorption spectroscopy. I. Calcium. Spectrochim Acta 16:259–271
17. Heinonen JK, Lahti RJ (1981) A new and convenient colorimetric determination of inorganic orthophosphate and its application to the assay of inorganic pyrophosphates. Anal Biochem 113:313–317
18. Termine JD, Posner AS (1966) Amorphous/crystalline interrelationship in bone mineral. Calcif Tissue Res 1:8–23
19. Roufosse AH, Landis WJ, Sabine WK, Glimcher MJ (1979) Identification of brushite in newly deposited bone mineral from embryonic chicks. J Ultrastruct Res 68:235–255
20. Bellows CG, Aubin JE, Heersche JNM (1991) Initiation and progression of mineralization of bone nodules formed in vitro: the role of alkaline phosphatase and organic phosphate. Bone Miner 14:27–40
21. Satomura K, Hiraiwa K, Nagasayama M (1991) Mineralized nodule formation in rat bone marrow stromal cell culture without β-glycerophosphate. Bone Miner 14:41–54
22. Khouja HI, Bevington A, Kamp GJ, Russell RGG (1990) Calcium and orthophosphate deposits in vitro do not imply osteoblast-mediated mineralization: mineralization by beta glycerophosphate in the absence of osteoblasts. Bone 11:385–391